Electronic Supplementary Information

What Factors Influence the Catalytic Activity of Iron-salan Complexes for Aerobic Oxidative Coupling of 2-Naphthols?

Kenji Matsumoto, Hiromichi Egami, Takuya Oguma, and Tsutomu Katsuki*[†]
Department of Chemistry, Faculty of Science, Graduate School and International Institute for Carbon-Neutral Energy Research (WPI-I^2CNER) , Kyushu University, Hakozaki, Higashi-ku, Fukuoka 812-8581, Japan.

General. The dinuclear iron(III)–salan and salen complexes (complexes **4**-**6**) and the mononuclear Fe(III)–salan complex with 3-bromo-2-naphtholate (complex **7**) were prepared according to the reported procedure.[1]

Complex **4**: Anal. Calc. for $C_{112}H_{86}Fe_2N_4O_6{\cdot}0.5H_2O$: C; 78.92, H; 5.14, N; 3.29, Found: C; 78.81, H; 5.29, N; 3.23.
Complex **5**: Anal. Calc. for $C_{96}H_{78}Fe_2N_4O_6{\cdot}1.5H_2O$: C; 75.74, H; 5.36, N; 3.68, Found: C; 75.70, H; 5.48, N; 3.92.
Complex **6**: Anal. Calc. for $C_{136}H_{92}Fe_2N_4O_5$: C; 82.75, H; 4.70, N; 2.84, Found: C; 82.47, H; 4.80, N; 2.81.
Complex **7**: Anal. Calc. for $C_{78}H_{58}Br_1Fe_1N_2O_4{\cdot}H_2O$: C; 75.49, H; 4.87, N; 2.26, Found: C; 75.35, H; 4.96, N; 2.41.

X-ray crystallography. The X-ray crystallographic analyses of the di-*μ*-hydroxo dinuclear iron(salan) complex **1** and the mononuclear iron(salan)(naphthoxo) complex **7** have been reported previously.[1] Single crystals of the di-*μ*-hydroxo dinuclear iron(salan) complexes **3-5** and *μ*-oxo dinuclear iron(salen) complex **6** were obtained from the CH_2Cl_2-Et_2O-*n*-hexane (for complexes **4** and **6**) or the acetone-water (for complexes **3** and **5**) mixed solution by slow evaporation of the volatile component at room temperature. Regarding the mononuclear iron(salan)(naphthoxo) complex **8** and the naphthoxo bridged dinuclear iron(salan) complex **9**, these single crystals were prepared by slow diffusion of *n*-hexane (for complex **8**) or *n*-heptane (for complex **9**) layered on the CH_2Cl_2 solution containing a large excess of corresponding ancillary ligands (1-bromo-2-naphthol for complex **8** and 6-bromo-2-naphthol for complex **9**) at 1 °C. Single crystals of the mononuclear iron(salen)(naphthoxo) complex **10** were formed from the CH_2Cl_2-MeCN-EtOH mixed solution of **6** in the presence of a large excess of 3-bromo-2-naphthol by slow evaporation of the volatile component at room temperature. A single crystal was mounted on a grass fiber with silicon grease and placed in the nitrogen gas stream cooled to 100 K. An X-ray diffraction measurement was made on a Bruker SMART APEX II diffractometer equipped with APEX II 4K CCD area detector, a graphite monochromator and a rotating-anode X-ray tube (Mo *K*α radiation, λ = 0.71073 Å) focused with Helios multilayer optics for Mo *K*α radiation, operating at 50 kV and 24 mA. The data collection was performed by the APEX2 software program.[2] The cell refinement and the data reduction were carried out using the program SAINT-NT.[3] The absorption correction was used by the SADABS program.[4] The structures were solved by direct methods and refined by full matrix least-squares based on all data using F^2 with program SHELXLTL.[5] All non-hydrogen atoms except for a part of solvent molecules were refined anisotropically. The hydrogen atoms attached to the carbon atoms were placed in calculated positions and refined using a riding model. The hydrogen atoms bonded to the nitrogen atoms were placed from the difference map and refined with geometrical and isotropic displacement parameters. Although most of complexes have showed high *w*R2 values, this is attributed to disordered atoms and/or unassignable residual peaks. Molecular plot was obtained with the program Mercury[6] and ORTEP-3[7]. CCDC 854405–854411 contains the supplementary crystallographic data for this paper. These data can be obtained free of charge from The Cambridge Crystallographic Data Centre via www.ccdc.ac.jk/data_request.cif.

References

(1) (a) H. Egami, T. Katsuki, *J. Am. Chem. Soc.* 2009, **131**, 6082–6083. (b) H. Egami, K. Matsumoto, T. Oguma, T. Kunisu, T. Katsuki, *J. Am. Chem. Soc.* 2010, **132**, 13633–13635.

(2) Bruker APEX2, Version 2008.5-0; Bruker AXS Inc.: Madison, WI (USA), 2005.

(3) Bruker SAINT-NT (includes XPREP and SADABS), Version 6.0; Bruker AXS Inc.: Madison, WI (USA), 2005.

(4) G. M. Sheldrick, SADABS, Program for Empirical Absorption Correction of Area Detector Data, University of Göttingen (Germany), 1996.

(5) (a) Bruker SHELXTL (includes XS, XL, XP, and XShell), Version 5.1, Bruker AXS INC.: Madison, WI (USA), 1997. (b) Sheldrick, G. M. *Acta Cryst.* 2008, **A64,** 112-122.

(6) (a) Mercury CSD 2.0: C. F. Macrae, I. J. Bruno, J. A. Chisholm, P. R. Edgington, P. McCabe, E. Pidcock, L. Rodriguez-Monge, R. Taylor, J. van de Streek, P. A. Wood, *J. Appl. Cryst.* 2008, **41**, 466-470. (b) Mercury: C. F. Macrae, P. R. Edgington, P. McCabe, E. Pidcock, G. P. Shields, R. Taylor, M. Towler, J. van de Streek, *J. Appl. Cryst.* 2006, **39**, 453-457. (c) I. J. Bruno, J. C. Cole, P. R. Edgington, M. K. Kessler, C. F. Macrae, P. McCabe, J. Pearson, R. Taylor, *Acta Cryst.* 2002, **B58**, 389-397. (d) R. Taylor, C. F. Macrae, *Acta Cryst.* 2001, **B57**, 815-827.

(7) ORTEP-3 for Windows: L. J. Farrugia *J. Appl. Crystallogr.* 1997, **30**, 565.

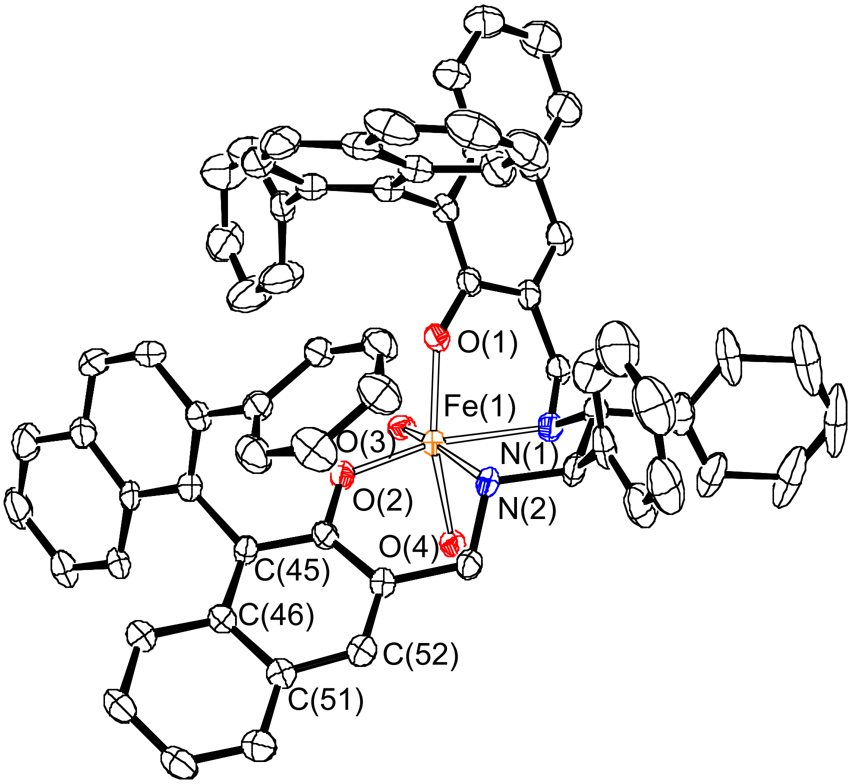

Fig. S1 Asymmetric unit of complex **1**. Ellipsoids drawn at the 50% probability level. All hydrogen atoms and solvent molecules are omitted for clarity. The C(45)–C(46)–C(51)–C(52) dihedral angle is 6.31°.

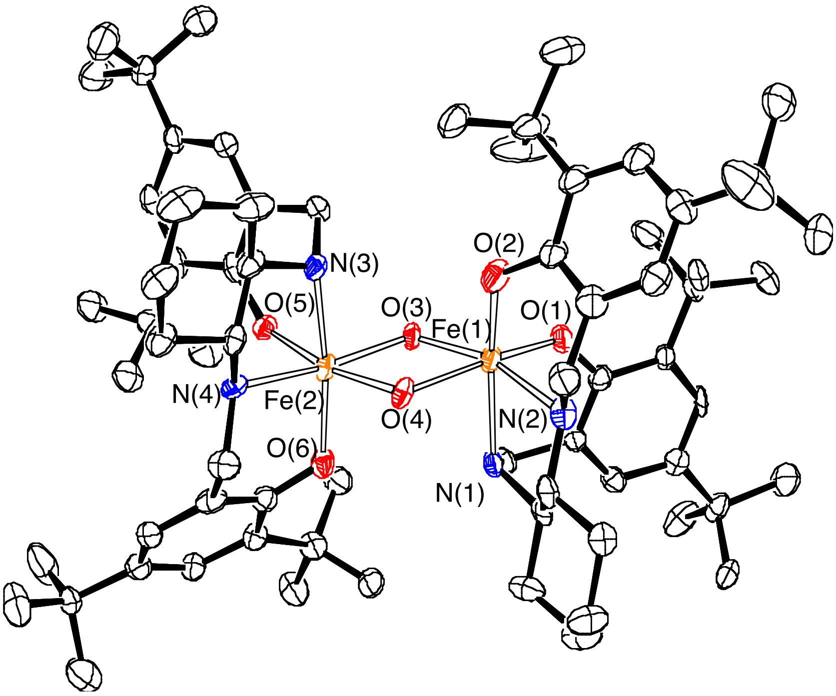

Fig. S2 Molecular structure of complex **3**. Ellipsoids drawn at the 50% probability level. All hydrogen atoms and solvent molecules are omitted for clarity.

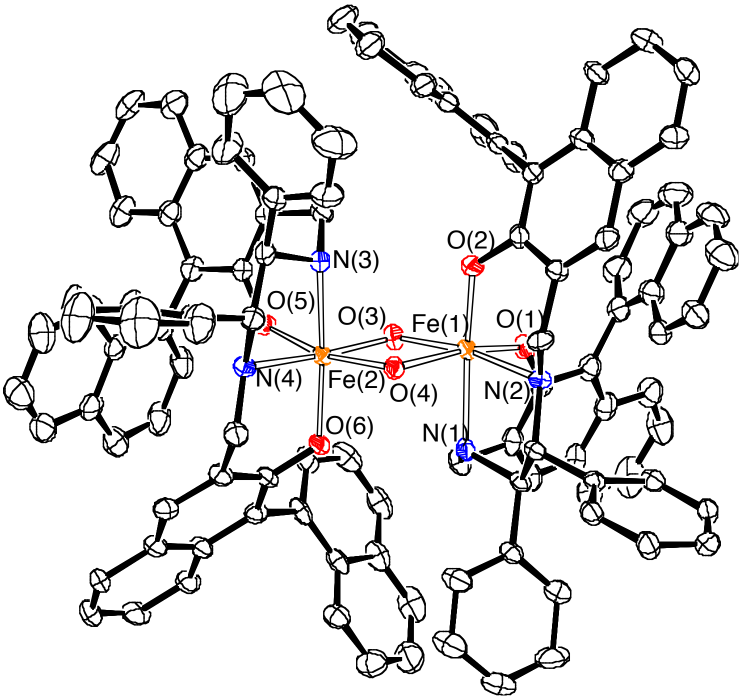

Fig. S3 Molecular structure of complex **4**. Ellipsoids drawn at the 50% probability level. All hydrogen atoms and solvent molecules are omitted for clarity.

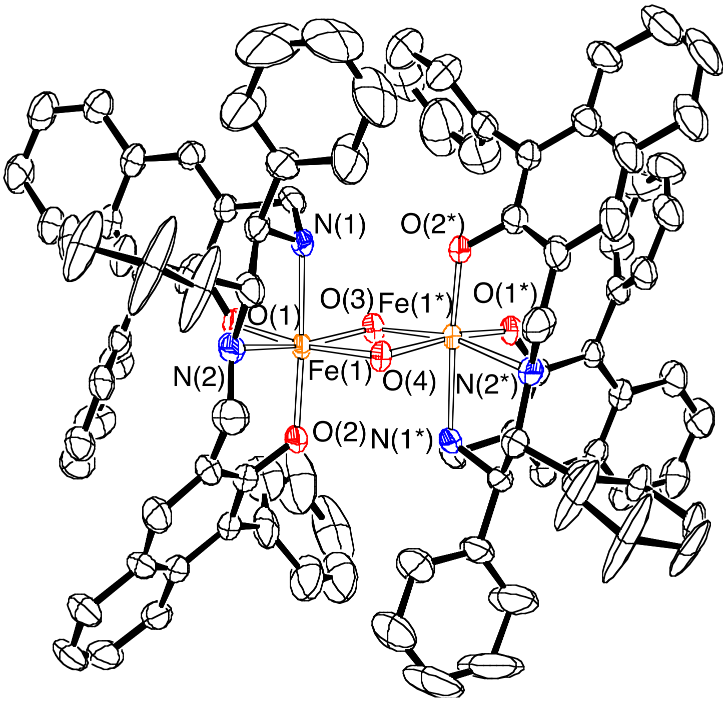

Fig. S4 Molecular structure of complex **5**. Ellipsoids drawn at the 50% probability level. All hydrogen atoms, solvent molecules and disordered atoms are omitted for clarity.

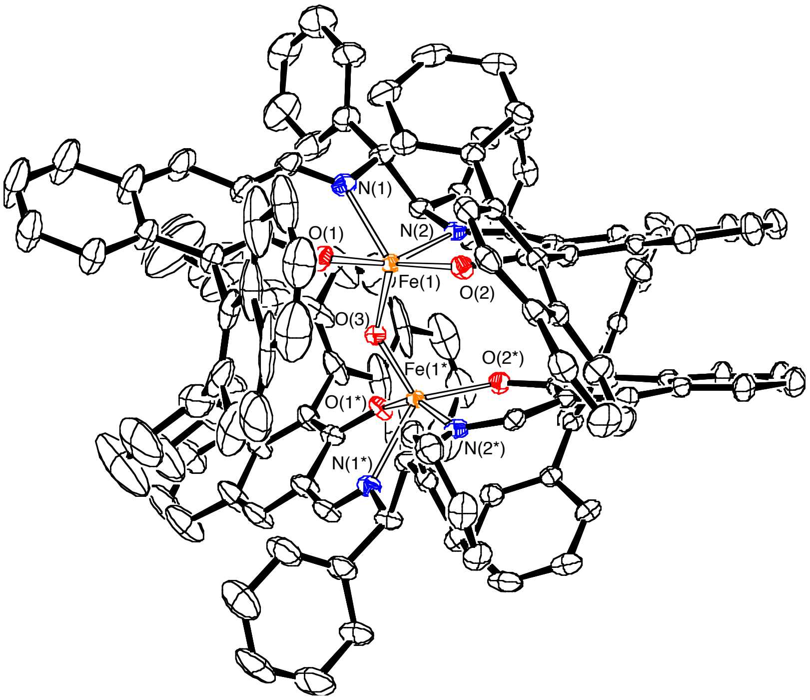

Fig. S5 Molecular structure of complex **6**. Ellipsoids drawn at the 50% probability level. All hydrogen atoms are omitted for clarity.

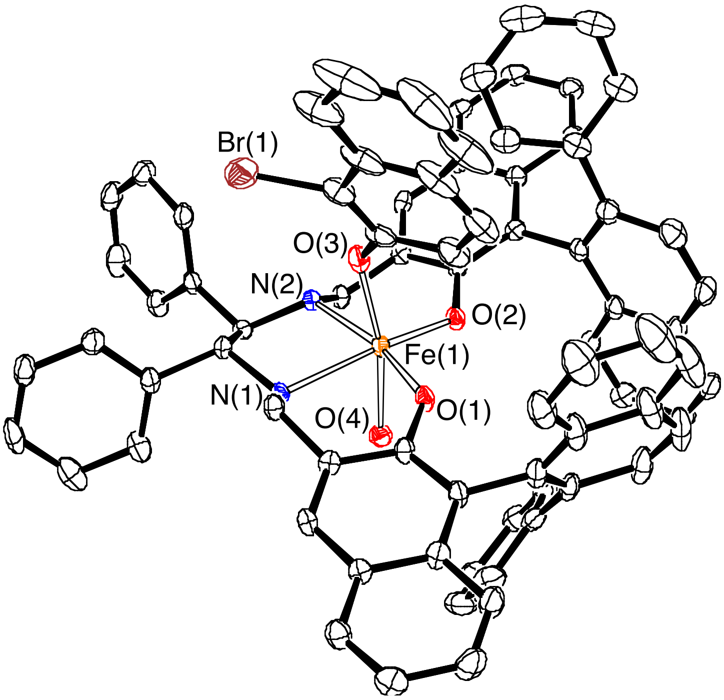

Fig. S6 Molecular structure of complex **8**. Ellipsoids drawn at the 50% probability level. All hydrogen atoms and solvent molecules are omitted for clarity.

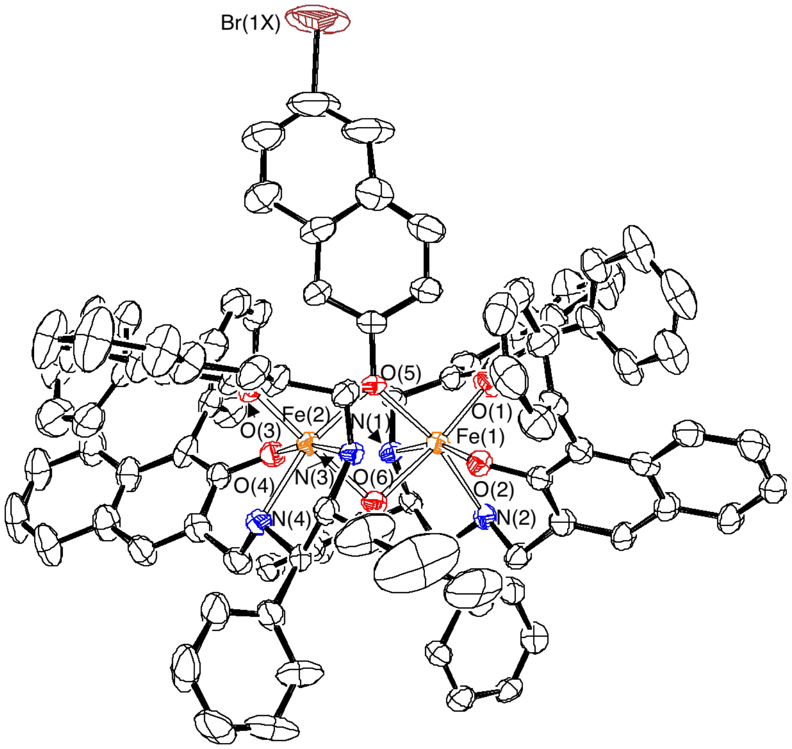

Fig. S7 Molecular structure of complex **9**. Ellipsoids drawn at the 50% probability level. All hydrogen atoms, solvent molecules and disordered atoms are omitted for clarity.

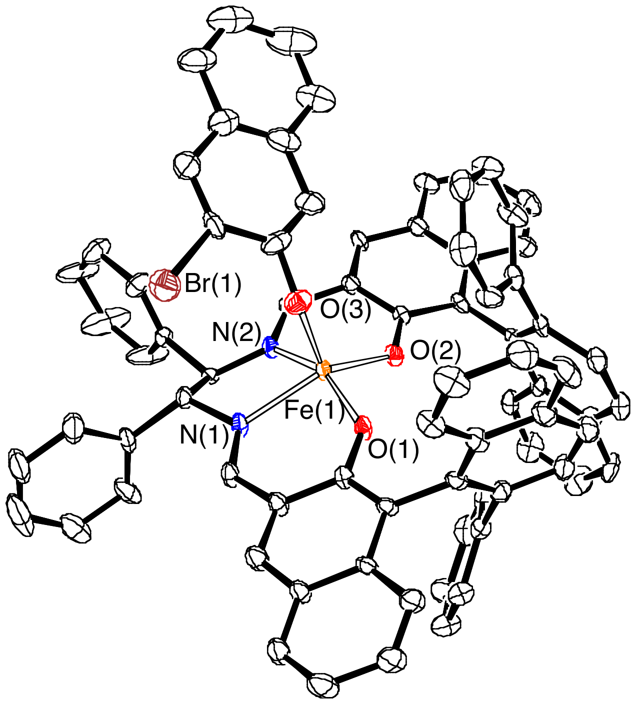

Fig. S8 Molecular structure of complex **10**. Ellipsoids drawn at the 50% probability level. All hydrogen atoms and solvent molecules are omitted for clarity.

Table S1 Crystallographic data of dinuclear iron(III)–salan and salen complexes.

compound	**1**·4$(C_2H_5)_2O$	2(**3**)·$(CH_3)_2CO$	**4**·CH_2Cl_2·2H_2O	**5**·2$(CH_3)_2CO$·H_2O	**6**	**9**·0.5(6-Br-2-NpOH)
formula	$C_{152}H_{142}Fe_2N_4O_{10}$	$C_{147}H_{234}Fe_4N_8O_{13}$	$C_{113}H_{92}Cl_2Fe_2N_4O_8$	$C_{102}H_{92}Fe_2N_4O_9$	$C_{136}H_{92}Fe_2N_4O_5$	$C_{111}H_{86.5}Br1.5Fe_2N_4O_{6.5}$
fw	2296.40	2544.82	1816.51	1629.50	1973.84	1811.91
crystal size (mm)	0.20 × 0.20 × 0.18	0.20 × 0.10 × 0.05	0.30 × 0.13 × 0.03	0.25 × 0.13 × 0.08	0.15 × 0.15 × 0.20	0.38 × 0.25 × 0.08
crystal color	deep purple	red	purple	red purple	red	dark purple
crystal description	block	plate	plate	block	block	block
crystal syst	tetragonal	orthorhombic	monoclinic	monoclinic	tetragonal	orthorhombic
space group	$P4_32_12$	$P2_12_12_1$	$P2_1$	$C2$	$P4_32_12$	$P2_12_12_1$
a (Å)	15.1812(18)	13.0266(13)	12.5225(14)	26.435(4)	18.3252(10)	13.6693(14)
b (Å)	15.1812(18)	19.7736(19)	25.289(3)	12.5897(17)	18.3252(10)	25.349(3)
c (Å)	52.476(6)	28.953(3)	15.7743(18)	18.562(5)	37.083(4)	27.020(3)
α (°)	90	90	90	90	90	90
β (°)	90	90	95.270(2)	125.3570(10)	90	90
γ (°)	90	90	90	90	90	90
V (Å^3)	12094(2)	7457.9(13)	4974.3(10)	5038.1(16)	12452.8(17)	9362.6(17)
Z	4	2	2	2	4	4
T (K)	100	100	100	100	100	100
ρ_{calcd}(Mg m^{-3})	1.261	1.133	1.213	1.074	1.053	1.285
μ(Mo$K\alpha$), (mm^{-1})	0.305	0.439	0.403	0.341	0.284	1.008
F(000)	4856	2760	1896	1712	4112	3748
reflns collected/independent reflns (R_{int})	68659/13858 (0.0346)	39867/16754 (0.0530)	57214/22598 (0.0419)	28940/11455 (0.0207)	71059/14313 (0.0408)	53205/21307 (0.0378)
data/ restraints/ parameters	13858/ 0/ 716	16754/ 0/ 819	22598/ 1/ 1160	11455/ 3/ 569	14313/ 0/ 663	21307/ 0/ 1111
R1 ($I > 2\sigma(I)$, all data)	0.0688, 0.0817	0.0873, 0.1282	0.0889, 0.1165	0.0840, 0.0925	0.0802, 0.0988	0.1061, 0.1372
wR2 ($I > 2\sigma(I)$, all data)	0.1985, 0.2076	0.1792, 0.1920	0.2473, 0.2713	0.2407, 0.2520	0.2318, 0.2530	0.2848, 0.3152
goodness of fit	1.106	1.183	1.030	1.106	1.141	1.045
Flack pram / Friedel pairs	0.01(2)	0.03(2)	0.009(19)	0.01(2)	0.00(2)	0.02(2)
residual density, (e Å^{-3})	+1.546/–0.712	+0.878/–0.773	+2.561/–0.513	+1.515/–0.543	+1.271/–0.464	+5.648/–1.506

Table 2 Crystallographic data of mononuclear iron(III)–salan and salen complexes.

compound	**7**·$(CH_3)_2CO\cdot H_2O$	**8**·$CH_2Cl_2\cdot H_2O$	**10**·EtOH
formula	$C_{81}H_{66}Br_1Fe_1N_2O_6$	$C_{79}H_{62}Br_1Cl_2Fe_1N_2O_5$	$C_{80}H_{58}Br_1Fe_1N_2O_4$
fw	1299.12	1325.97	1247.04
crystal size (mm)	0.10 × 0.08 × 0.05	0.18 × 0.15 × 0.10	0.20 × 0.13 × 0.10
crystal color	dark purple	dark purple	dark brown
crystal description	block	block	block
crystal syst	orthorhombic	orthorhombic	monoclinic
space group	$P2_12_12_1$	$P2_12_12_1$	$P2_1$
a (Å)	13.8731(11)	14.237(2)	14.5514(16)
b (Å)	20.8602(17)	19.981(3)	16.0909(17)
c (Å)	21.8492(18)	22.218(3)	15.7159(17)
α (°)	90	90	90
β (°)	90	90	112.0170(10)
γ (°)	90	90	90
V (Å^3)	6323.1(9)	6320.1(17)	3411.4(6)
Z	4	4	2
T (K)	100	100	100
ρ_{calcd}(Mg m^{-3})	1.365	1.394	1.214
μ(Mo$K\alpha$), (mm^{-1})	0.930	1.012	0.857
F(000)	2700	2740	1290
reflns collected/independent reflns (R_{int})	36253/14310 (0.0357)	36196/14367 (0.0317)	39325/15559 (0.0285)
data/ restraints/ parameters	14310/ 0/ 830	14367/ 0/ 827	15559/ 1/ 793
R1 ($I > 2\sigma(I)$, all data)	0.0427, 0.0607	0.0444, 0.0561	0.0986, 0.1097
wR2 ($I > 2\sigma(I)$, all data)	0.0947, 0.1022	0.1093, 0.1157	0.2757, 0.2880
goodness of fit	0.998	1.013	1.259
Flack pram / Friedel pairs	–0.008(6)	0.001(6)	0.023(12)
residual density, (e Å^{-3})	+0.725/–0.558	+0.866/–0.519	+6.416/–0.682

Table S3 Selected geometric parameters of dinuclear Fe(III)–salan and salen complexes.

compound	$\mathbf{1}\cdot4(C_2H_5)_2O$	$2(\mathbf{3})\cdot(CH_3)_2CO$	$\mathbf{4}\cdot CH_2Cl_2\cdot2H_2O$	$\mathbf{5}\cdot2(CH_3)_2CO\cdot H_2O$	**6**	$\mathbf{9}\cdot0.5$(6-Br-2-NpOH)
bond lengths (Å)						
Fe(1)–N(1)	2.165(3)	2.165(5)	2.185(5)	2.172(3)	2.169(3)	2.221(6)
Fe(1)–N(2)	2.172(3)	2.199(5)	2.176(5)	2.184(4)	2.100(3)	2.159(6)
Fe(1)–O(1)	1.922(2)	1.914(3)	1.914(4)	1.910(3)	1.918(3)	1.897(5)
Fe(1)–O(2)	1.910(2)	1.931(4)	1.910(4)	1.906(3)	1.913(3)	1.934(5)
Fe(1)–O(3)	1.990(2)	1.983(3)	1.971(4)	1.956(3)	1.8038(15)	2.008(5) (Fe(1)–O(5))
Fe(1)–O(4)	2.077(2)	2.095(3)	2.092(4)	2.031(3)	–	2.058(5) (Fe(1)–O(6))
Fe(1*)···N(1*)	[a]	2.203(5) (Fe(2)–N(3))	2.199(5) (Fe(2)–N(3))	[a]	[a]	2.177(6) (Fe(2)–N(3))
Fe(1*)···N(2*)	[a]	2.190(4) (Fe(2)–N(4))	2.185(5) (Fe(2)–N(4))	[a]	[a]	2.216(6) (Fe(2)–N(4))
Fe(1*)···O(1*)	[a]	1.914(3) (Fe(2)–O(5))	1.901(4) (Fe(2)–O(5))	[a]	[a]	1.891(4) (Fe(2)–O(3))
Fe(1*)···O(2*)	[a]	1.926(4) (Fe(2)–O(6))	1.927(4) (Fe(2)–O(6))	[a]	[a]	1.929(4) (Fe(2)–O(4))
Fe(1*)···O(3)	[a]	1.988(3) (Fe(2)–O(3))	1.958(4) (Fe(2)–O(3))	[a]	[a]	2.042(5) (Fe(2)–O(5))
Fe(1*)···O(4)	[a]	2.059(3) (Fe(2)–O(4))	2.055(4) (Fe(2)–O(4))	[a]	[a]	2.033(5) (Fe(2)–O(6))
Fe(1)···Fe(1*)	3.205	3.182 (Fe(1)···Fe(2))	3.107 (Fe(1)···Fe(2))	3.088	3.396	3.134 (Fe(1)···Fe(2))
N(1)···O(2*)	3.531	3.299 (N(1)···O(6))	3.147 (N(1)···O(6))	3.193	–	3.208 (N(1)–O(4))
N(1*)···O(2)	[a]	3.397 (N(3)···O(2))	3.237 (N(3)···O(2))	[a]	–	3.052 (N(3)–O(2))
bond angles (°)						
N(1)–Fe(1)–N(2)	77.59(12)	77.6(2)	79.39(18)	78.89(16)	75.22(14)	78.5(2)
N(1)–Fe(1)–O(1)	83.62(11)	86.94(19)	86.34(18)	86.95(15)	85.44(13)	86.3(2)
N(2)–Fe(1)–O(2)	83.28(11)	88.0(2)	89.00(18)	89.85(14)	86.85(13)	91.4(2)
O(3)–Fe(1)–O(4)	75.89(11)	76.38(13)	78.58(16)	78.39(11)	–	79.37(18) (O(5)–Fe(1)–O(6))
N(1*)–Fe(1*)–N(2*)	[a]	77.11(18) (N(3)–Fe(2)–N(4))	78.70(18) (N(3)–Fe(2)–N(4))	[a]	[a]	77.4(2) (N(3)–Fe(2)–N(4))
N(1*)–Fe(1*)–O(1*)	[a]	86.48(18) (N(3)–Fe(2)–O(5))	85.69(19) (N(3)–Fe(2)–O(5))	[a]	[a]	90.0(2) (N(3)–Fe(2)–O(3))
N(2*)–Fe(1*)–O(2*)	[a]	88.58(17) (N(4)–Fe(2)–O(6))	87.39(18) (N(4)–Fe(2)–O(6))	[a]	[a]	88.5(2) (N(4)–Fe(2)–O(4))
O(3)–Fe(1*)–O(4)	[a]	77.12(13) (O(3)–Fe(2)–O(4))	79.79(16) (O(3)–Fe(2)–O(4))	[a]	[a]	79.18(18) (O(5)–Fe(2)–O(6))
Fe(1)–O(3)–Fe(1*)	107.24(16)	106.50(16) (Fe(1)–O(3)–Fe(2))	104.51(19) (Fe(1)–O(3)–Fe(2))	104.2(2)	140.6(2)	101.40(19) (Fe(1)–O(5)–Fe(2))
Fe(1)–O(4)–Fe(1*)	100.97(15)	99.98(15) (Fe(1)–O(4)–Fe(2))	97.06(17) (Fe(1)–O(4)–Fe(2))	98.97(19)	–	100.05(19) (Fe(1)–O(6)–Fe(2))

[a] Same value with corresponding bond length without asterisk.

Table S4 Selected geometric parameters of mononuclear Fe(III)–salan and salen complexes.

compound	**7**·$(CH_3)_2CO \cdot H_2O$	**8**·$CH_2Cl_2 \cdot H_2O$	**10**·EtOH
bond lengths (Å)			
Fe(1)–N(1)	2.188(2)	2.202(2)	2.120(4)
Fe(1)–N(2)	2.191(2)	2.171(2)	2.123(4)
Fe(1)–O(1)	1.8879(18)	1.872(2)	1.889(3)
Fe(1)–O(2)	1.9092(19)	1.927(2)	1.900(4)
Fe(1)–O(3)	1.962(2)	1.975(2)	1.864(5)
Fe(1)–O(1W) (O(4))	2.214(2)	2.214(2)	–
bond angles (º)			
N(1)–Fe(1)–N(2)	77.33(9)	78.16(9)	75.99(17)
N(1)–Fe(1)–O(1)	88.74(8)	88.94(9)	87.34(16)
N(2)–Fe(1)–O(2)	87.27(8)	88.57(9)	85.17(17)
O(1)–Fe(1)–O(2)	106.15(8)	103.80(9)	98.25(16)
O(3)–Fe(1)–O(1W) (O(4))	164.18(8)	166.48(9)	–

Electrochemistry. All cyclic voltammetries were carried out under the following conditions: CH_2Cl_2 solvent, 1 mM samples (ligands and Fe(III) complexes), 100 mM tetra-*n*-butylammonium hexafluorophosphate (^{n}Bu$_4$NPF$_6$) as supporting electrolyte, total volume 10 mL, a glassy carbon working electrode, an Ag^+/Ag reference electrode, a Pt wire counter electrode, sweep rate 100 mV/s, 3 cycles, at room temperature. ^{n}Bu$_4$NPF$_6$ was recrystallized from hot acetonitrile before use. Before the measurement, de-aeration of the solution was carried out using N_2 gas (through CH_2Cl_2) bubbling during at least 15 minutes. The voltammogram was taken by the CHI620 Electrochemical Analyzer (ALS). The potential value obtained for the Ag^+/Ag reference electrode scale was converted to the ferrocenium/ferrocene (Fc^+/Fc) scale using the redox potential of Fc^+/Fc obtained in the same condition as an internal reference.

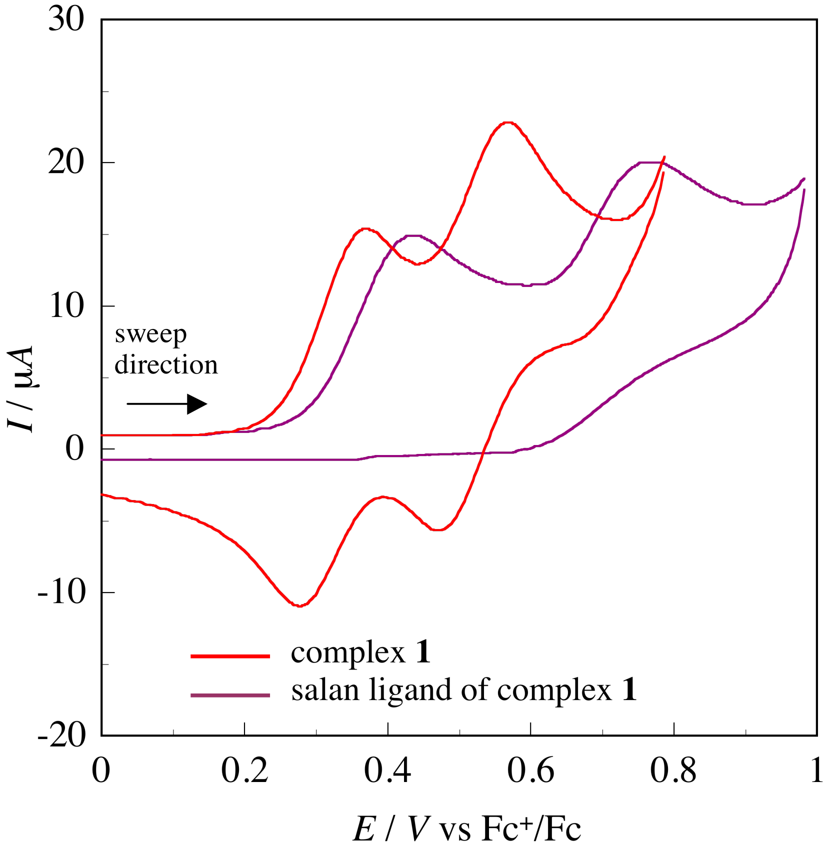

Fig. S9 Cyclic voltammogarms of complex **1** and its salan ligand.

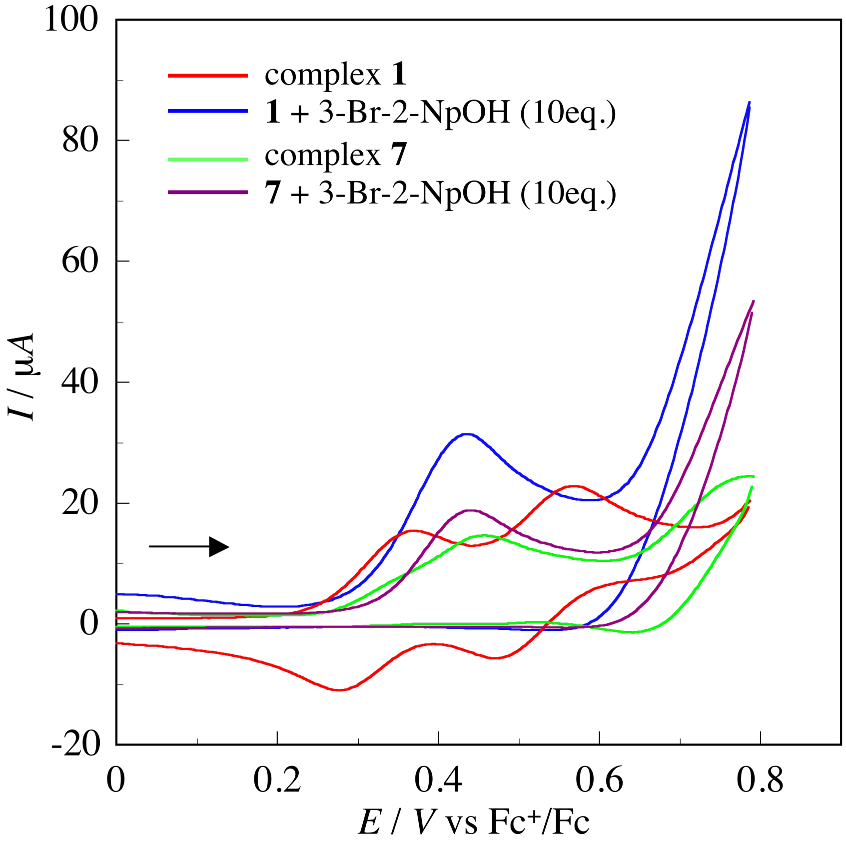

Fig. S10 Cyclic voltammogams of complex **1** and **7** before and after addition of 3-bromo-2-naphthol.

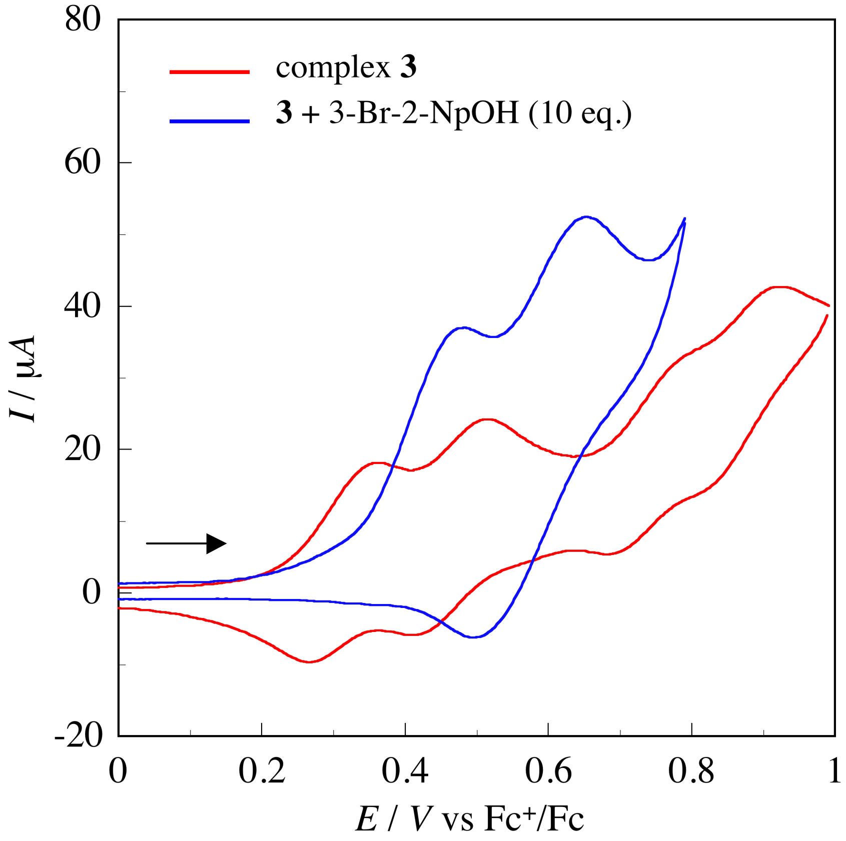

Fig. S11 Cyclic voltammogarms of complex **3** before and after addition of 3-bromo-2-naphthol.

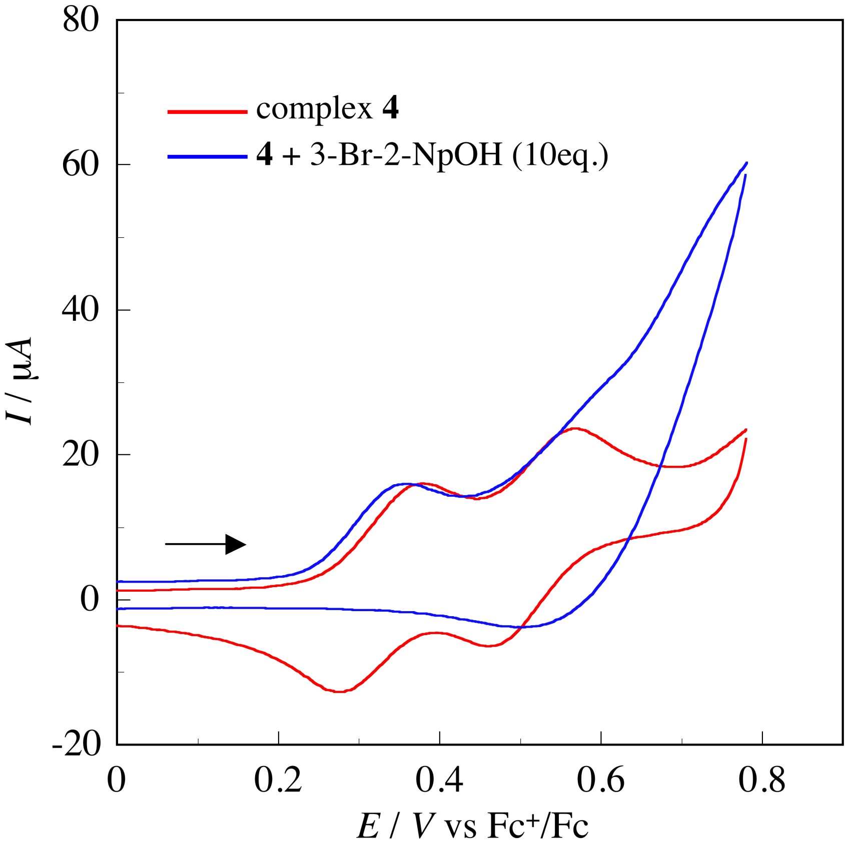

Fig. S12 Cyclic voltammogarms of complex **4** before and after addition of 3-bromo-2-naphthol.

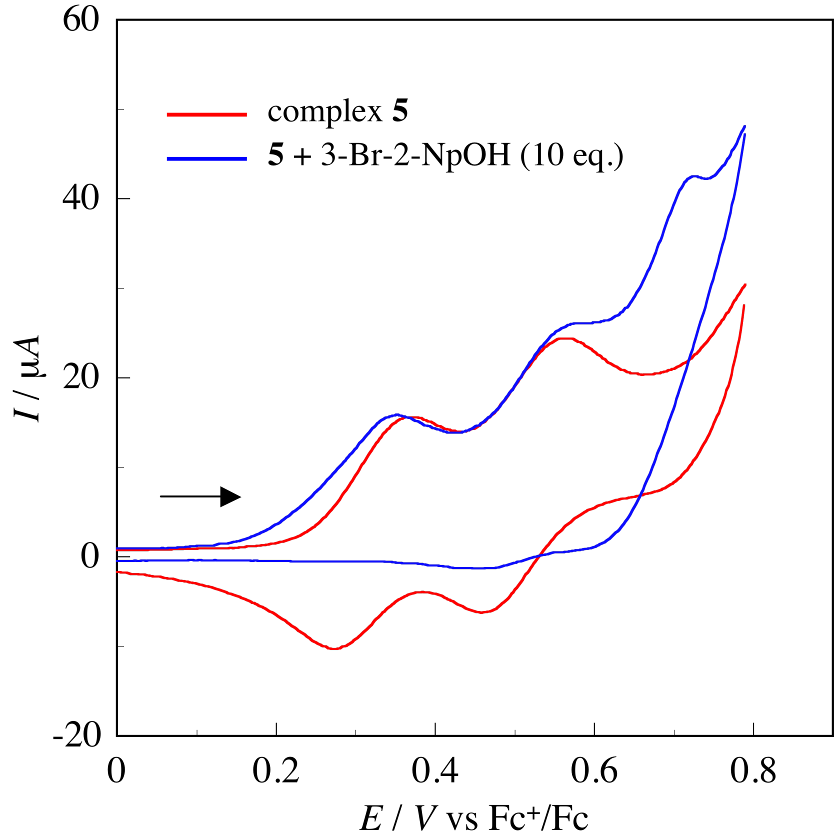

Fig. S13 Cyclic voltammogarms of complex **5** before and after addition of 3-bromo-2-naphthol.

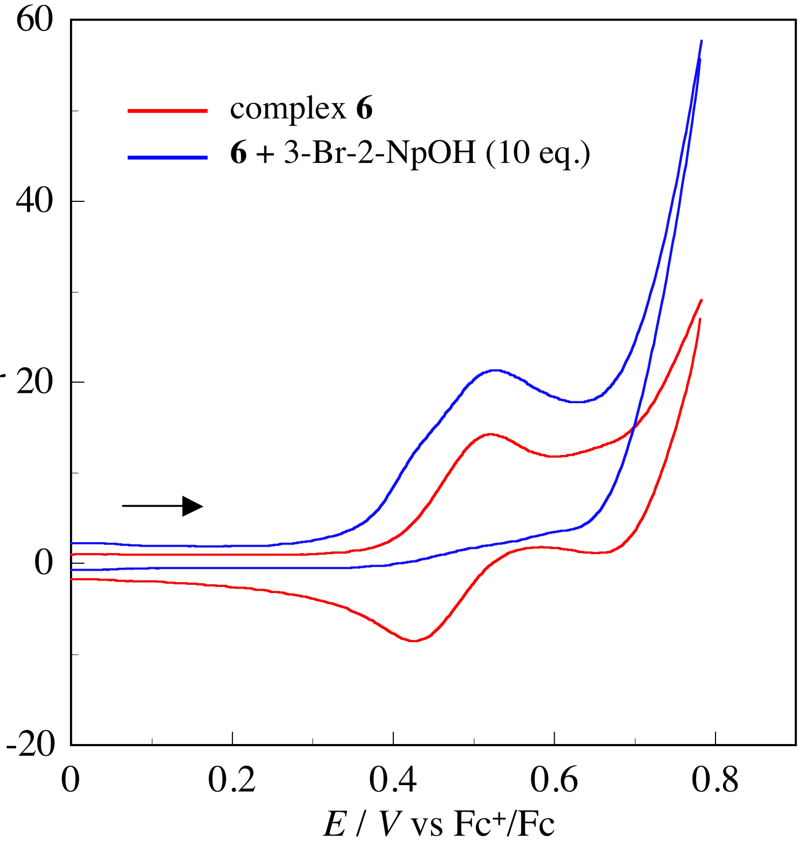

Fig. S14 Cyclic voltammogarms of complex **6** before and after addition of 3-bromo-2-naphthol.